Salidroside protects against intestinal barrier dysfunction in septic mice by regulating IL-17 to block the NF-κB and p38 MAPK signaling pathways

RONGXIN LIAO, PENG ZHAO, JIANMING WU and KEREN FANG

Center of Traditional Chinese Medicine Preventive Treatment, Integrated Hospital of Traditional Chinese Medicine, Southern Medical University, Guangzhou, Guangdong 510310, P.R. China

Received September 15, 2021; Accepted September 29, 2022

DOI: 10.3892/etm.2023.11788

Abstract. Sepsis is a systemic inflammatory response syndrome, mainly caused by infection or suspected infectious factors. The intestine is not only one of the most easily involved organs in the course of sepsis, but also the dynamic organ for the course of sepsis. The present study investigated the protective effect and mechanism of salidroside on intestinal barrier dysfunction of septic mice. Briefly, C57BL/6 mice were used to establish a septic model and then administered with salidroside. The ileum tissues of mice were examined by histopathological examination. Fluorescein isothiocyanate-dextran concentration was measured. IL-17, IL-6, IL-13 and TNF-α levels in ileum tissues and NF-κB and p38 MAPK activations were detected by ELISA and the expressions of NF-κB p65 and p38 MAPK protein with their phosphorylation and intestinal tight junction proteins were gauged by western blotting. The above assays were performed again to investigate the effect of anti-IL-17A and salidroside (160 mg/kg) alone or in combination. The septic model induced the ileum tissue injury, increased intestinal permeability and TNF-α, IL-17 and IL-6 levels, activated NF-κB and p38 MAPK pathways, promoted the expressions of NF-κB p65 and p38 MAPK and their phosphorylation, while suppressing the levels of IL-13 and intestinal tight junction proteins. Salidroside and anti-IL-17A partially reversed the above effects of septic model, which in combination further strengthened the reversing effect. Collectively, salidroside protected against intestinal barrier dysfunction in septic mice by downregulating IL-17 level to inhibit NF-κB and p38 MAPK signaling pathways, thus providing a new treatment direction.

Correspondence to: Dr Rongxin Liao, Center of Traditional Chinese Medicine Preventive Treatment, Integrated Hospital of Traditional Chinese Medicine, Southern Medical University, 13 Shiliugang Road, Haizhu, Guangzhou, Guangdong 510310, P.R. China
E-mail: chinalrx2021@163.com

Key words: sepsis, salidroside, IL-17, NF-κB signaling pathway, p38 mitogen-activated protein kinase signaling pathway

Introduction

Sepsis can be secondary to severe trauma, burn, infection and other clinical acute and critical diseases, manifested as systemic inflammatory response disorder and host autoimmune injury and can result in obvious hemodynamic disorder and multiple organ dysfunction. In the majority of cases, sepsis is a syndrome of circulatory, immune and metabolic dysfunction (1-3). The gut is the first organ to be affected in sepsis. The normal intestinal mucosal barrier is composed of mechanical, chemical, biological and immune barriers (4). Among them, the immune barrier serves a key role in maintaining the normal operation of the intestinal tract and preventing bacterial endotoxin translocation (4). The impairment of intestinal mucosal barrier function, especially the immune barrier damage, leads to immune inflammatory injury and bacterial translocation, which is an important cause of sepsis (5). Therefore, early protection of intestinal immune barrier function is a crucial consideration to prevent and control the occurrence and development of sepsis.

Rhodiola is a perennial herb, and exhibits beneficial effects on cognitive function, cardiovascular system and fatigue (6). *Rhodiola* contains more than 40 chemical constituents including alcohols, polysaccharides, ketones and phenolic compounds and a variety of amino acids and trace elements, with extremely complicated pharmacological activities (6). Salidroside, one of the most effective and active components extracted from *Rhodiola*, is a phenylethanol compound (7). In recent years, a number of studies have uncovered that salidroside not only has protective effects on the cardiovascular, cerebrovascular, immune and central nervous systems, but also possesses a number of pharmacological effects such as anti-inflammation and inhibiting cell apoptosis (8-12). Salidroside may be a potential candidate for the management of lung inflammation in cecal ligation and puncture (CLP)-induced endotoxemia and septic shock (13). However, there are few reports about the protective effect of salidroside on intestinal barrier dysfunction during sepsis.

T helper 17 (Th17) cells are a type of $CD4^+$ T cell which are named for their characteristic secretion of IL-17 (14). The IL-17 family consists of six members: IL-17A (IL-17), IL-17B, IL-17C,

IL-17D, IL-17E (IL-25) and IL-17F (15). IL-17 was discovered in 1993 has been considered as an important inflammatory factor, which has profound effects on the anti-infection defenses of the body, especially against extracellular bacteria and fungi (16). By virtue of its inflammatory properties, IL-17 is closely related to a number of autoimmune diseases, such as rheumatoid arthritis, multiple sclerosis, systemic lupus erythematosus, inflammatory bowel disease and psoriasis (17,18). Following treatment with IL-17 antibody, the inflammatory reaction and bone destruction in a collagen-induced arthritis mouse model were significantly reduced (19,20). In addition, targeting IL-17A can improve the dysmotility of the small intestine during sepsis (21) and IL-17-producing γδ T cells are important for the maintenance and protection of epithelial barriers in the intestinal mucosa (22). These studies illustrate that IL-17 may serve a vital role in the protection against intestinal barrier dysfunction during sepsis. In addition, IL-17 could activate p38 MAPK, ERK and NF-κB in various cells and diseases, including human salivary gland cells, human dental pulp fibroblasts, psoriasis and ischemic heart failure (23-26). MAPK and NF-κB pathways are related to sepsis-induced cardiac inflammation and dysfunction (27) and inhibiting activation of MAPK/NF-κB can safeguard against lipopolysaccharide-induced sepsis (28), indicating that MAPK and NF-κB pathways may be involved in the pathogenesis of sepsis. In addition, it has been noted that salidroside inhibits MAPK and NF-κB pathways (9,29).

Based on the above understandings, the present study constructed a sepsis mouse model to investigate the effects of salidroside and IL-17 on intestinal barrier dysfunction, so as to explore an approach for gaining clinical benefit.

Materials and methods

Ethics statement. All animal experiments, were performed in Nanfang Hospital following the guidelines of the China Council on Animal Care and Use and were permitted by the Committee of Experimental Animals of Nanfang Hospital (approval no. S201709024). Pain and discomfort to the animals were minimized.

Animals. A total of 80 SPF grade C57BL/6 mice (6-8 weeks old, weighing 18-22 g) were purchased from Vital River Laboratory Animal Technology Co. Ltd. and raised under the SPF barrier system of the Laboratory Animal Center of the Nanfang Hospital. The light cycle was 12-h light/12-h dark, and room temperature was maintained at 21-25˚C, with a humidity of 20-30%. The mice had free access to food and water and were subjected to the experiment ~3 weeks after acclimation.

Establishment and administration of the animal model. Salidroside (CAS: 10338-51-9; cat. no. SMB00072; purity ≥95%) was purchased from MilliporeSigma. In the sham and salidroside (320 mg/kg) groups, only the mouse abdominal cavity was opened and the cecum was turned over and then closed layer by layer without intestinal puncture and ligation. The sepsis mice models were established using the CLP method. The main steps were: The mice were fasted 12 h before operation and drank freely; 2% pentobarbital sodium (cat. no. P-010; Supelco Inc.) was injected intraperitoneally into mice at 40 mg/kg for abdominal anesthesia; a 1.5 cm longitudinal incision was made in the middle of the mouse abdomen; the skin and muscle layers were cut layer by layer; the abdominal cavity was opened to expose the cecum; the cecum was ligated and punctured; and the intestine was ligated from ileocecum to 1/3 of cecum end with sterile silk thread (cat. no. BS0117; 4#; Changzhou Huawei Medical Supplies Co., Ltd.). A 21G sterile needle was used to penetrate the intestinal tube and a small amount of contents were gently squeezed out to ensure smooth perforation. After the abdomen was sutured, the mice in each group were injected subcutaneously with 5 ml/100 g normal saline for anti-shock therapy.

Mice in model, model + salidroside (80 mg/kg), model + salidroside (160 mg/kg) and model + salidroside (320 mg/kg) groups were intraperitoneally injected with salidroside dissolved in saline according to the dosage of 80, 160 and 320 mg/kg (30,31) within 30 min after the end of modeling. The corresponding volume of normal saline was injected into mice in the sham group and salidroside (320 mg/kg) groups.

Experimental grouping. Mice were randomly divided to eight groups, with 10 mice in each group: Sham group (mice were treated according to the above conditions); salidroside (320 mg/kg) group (mice treated as sham group were additionally intraperitoneally injected with 320 mg/kg salidroside); model group (septic model group); model + salidroside (80 mg/kg) group (mice were intraperitoneally injected with 80 mg/kg salidroside after modeling); model + salidroside (160 mg/kg) group (mice were intraperitoneally injected with 160 mg/kg salidroside after modeling); model + salidroside (320 mg/kg) group (mice were intraperitoneally injected with 320 mg/kg salidroside after modeling); model + anti-IL-17A group [mice were intraperitoneally injected with recombinant anti-IL-17A (cat. no. MAB421; R&D Systems, Inc.) at the dose of 5 mg/kg 6 h before modeling]; and model + salidroside 160 + anti-IL-17A group [mice were intraperitoneally injected with recombinant anti-IL-17A (cat. no. MAB421; R&D Systems, Inc.) at the dose of 5 mg/kg 6 h before modeling and then intraperitoneally injected with 160 mg/kg salidroside after modeling].

Histopathological examination. The mice were euthanized by cervical dislocation under 2% pentobarbital (40 mg/kg) anesthesia 24 h after surgery. The ileum tissues of the mice were collected, fixed with 4% paraformaldehyde fixative solution for 24 h at 4˚C, dehydrated with an increasing alcohol gradient (75, 85, 95 and 100%), cleared with xylene, routinely embedded in paraffin and sliced into serial cross sections. The 5 μm ileum tissue sections were stained with hematoxylin (cat. no. H3136; MilliporeSigma) for 10 min followed by staining with eosin (cat. no. E4009; MilliporeSigma) for 1 min and toluidine blue (cat. no. 89640; MilliporeSigma) for 10 min at room temperature to observe pathological and morphological changes.

Determination of fluorescein isothiocyanate-dextran (FD4) concentration. At 24 h after modeling, the mouse abdominal cavity was opened and the ileum (the segment with abundant mesenteric blood vessels) was taken and ligated at both ends. The ileum was cut from the loose knot and ligation site and washed with PBS. The free intestinal segment was tied tightly. Then 0.5 ml of FD4 solution (10 mg/ml) was injected to make

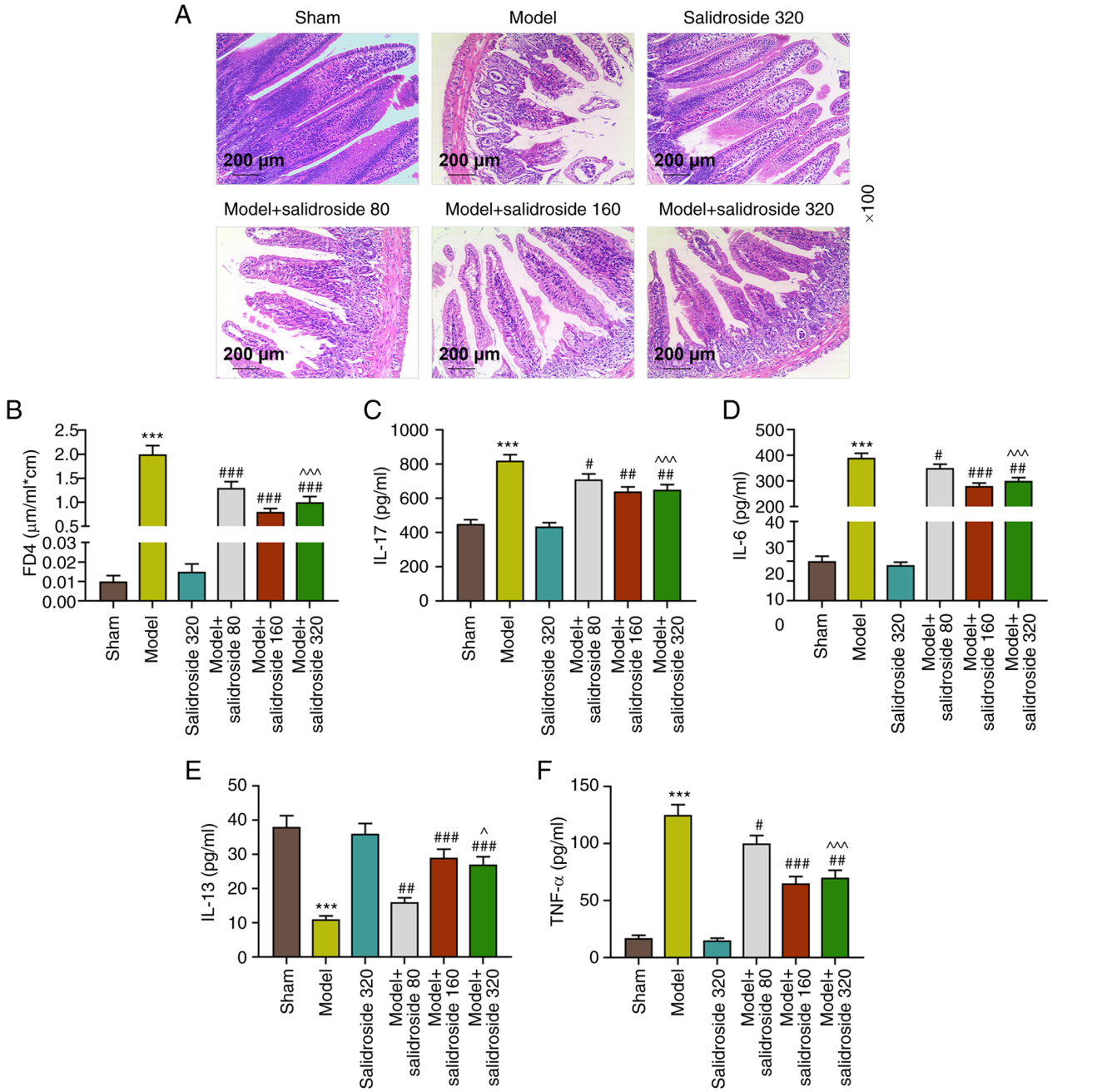

Figure 1. Salidroside affects the ileum tissue injury and intestinal permeability induced by a septic model and regulates ileum tissue cytokines. (A) The ileum tissues of mice were examined by histopathological examination. (B) FD4 concentration was measured by fluorospectrophotometer to detect intestinal permeability. (C-F) The cytokine levels of (C) IL-17, (D) IL-6, (E) IL-13 and (F) TNF-α in ileum were detected by ELISA. The data are presented as the mean ± standard deviation of three independent experiments; ***P<0.001 vs. sham; #P<0.05; ##P<0.01; ###P<0.001 vs. model; ^P<0.05; ^^^P<0.001 vs. salidroside (320 mg/kg). FD4, fluorescein isothiocyanate-dextran.

FD4 enter the blood circulation through mesonic vessel. After 30 min, heart blood samples were harvested and placed into centrifuge tube for 10 min centrifugation at 10,000 x g at 4˚C, based on which the samples were transferred to a new centrifuge tube, diluted at 1:8 and inoculated to a 96-well plate (100 μl/well). FD4 concentration in blood samples was determined by a fluorospectrophotometer (F-7100; Hitachi, Ltd.).

Enzyme-linked immune sorbent assay (ELISA). Ileum tissues were homogenized for ELISA. Homogenization was performed in ice-cold homogenate buffer, containing 10 mM HEPES (pH 7.9), 10 mM KCl, 2 mM $MgCl_2$, 0.1 mM EDTA, 1.0 mM dithiothreitol (DTT) and 0.5 mM phenylmethanesulfonylfluoride (PMSF). The homogenates were centrifuged at 3,000 x g for 15 min at 4˚C. The supernatants were subsequently stored at -70˚C before use. Then TNF-α, IL-6, IL-13 and IL-17 levels in ileum tissues were measured using ELISA kits (TNF-α; cat. no. RAB0477; MilliporeSigma; IL-6 and IL-13; cat. nos. KMC0061 and KMC2221; Invitrogen; Thermo Fisher Scientific, Inc.; IL-17; cat. no. 860.070.048; Diaclone Research, SAS) according to the instructions of the manufacturers. The protein levels of TNF-α, IL-6, IL-13 and IL-17 were expressed as pg/ml.

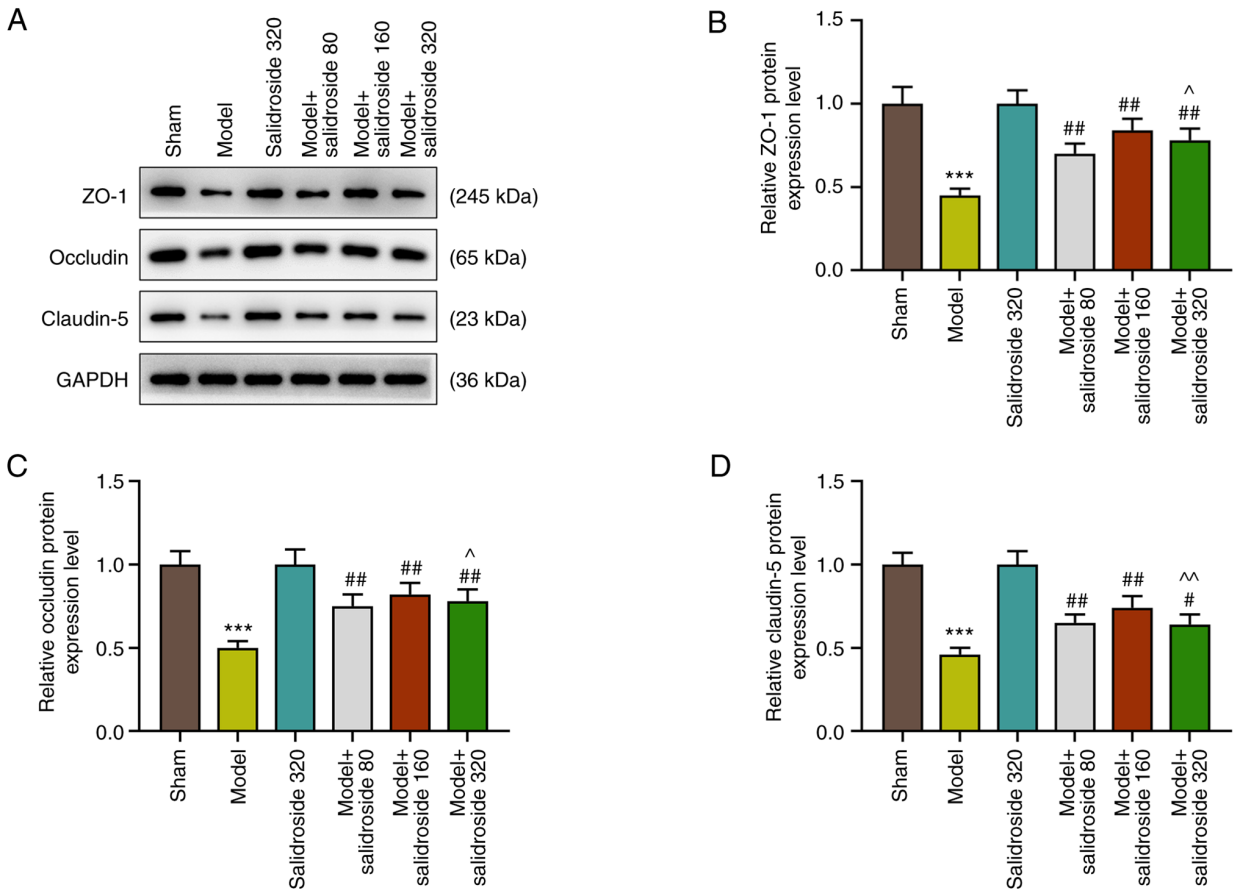

Figure 2. Salidroside attenuates the decrease in the levels of intestinal tight junction proteins in a septic model. (A) The levels of intestinal tight junction proteins (B) ZO-1, (C) occludin and (D) claudin-5 were detected by western blotting. GAPDH was served as the internal reference. The data are presented as the mean ± standard deviation of three independent experiments. ***P<0.001 vs. sham; $^{\#\#}$P<0.01 vs. model; $^{\wedge}$P<0.05; $^{\wedge\wedge}$P<0.01 vs. salidroside (320 mg/kg). ZO-1, zonula occludens-1.

Analysis of NF-κB and p38 MAPK signaling activation. The activation of NF-κB and p38 MAPK signaling was measured by DNA-binding activity with TransAM Transcription Factor ELISA kits (Active Motif, Inc.). Nuclear extracts were collected using a Nuclear Extract kit (Active Motif, Inc.). Proteins were quantified in line with the BCA method and subjected to an ELISA-based TransFactor assay.

Western blotting. Radioimmunoprecipitation assay lysis buffer (cat. no. P0013K, Beyotime, China) was applied to extract the total protein from ileum tissues. Protein content was quantified utilizing the BCA assay reagent kit (cat. no. C503021, Sangon, China). The SDS-PAGE (with 6-10% gels) was used to separate the 30-μg protein samples and the separated protein was transferred to the PVDF membrane (cat. no. IPFL00010; MilliporeSigma) which was then blocked in 5% skimmed milk for 2 h at room temperature. The membrane was subsequently incubated with primary antibodies at 4˚C overnight. The primary antibodies were as follows: NF-κB p65 (Abcam; Rabbit; 1:1,000 dilution; cat. no. ab207297; 65 kDa), phosphorylated (p)-NF-κB p65 (CST; Rabbit; 1:1,000 dilution; cat. no. 3033; 65 kDa), zonula occludens-1 (ZO-1; Abcam; Rabbit; 1:1,000 dilution; cat. no. ab216880; 245 kDa) and claudin-5 (Abcam; Rabbit; 1:1,000 dilution; cat. no. ab13125; 23 kDa), occluding (CST; Rabbit; 1:1,000 dilution; cat. no. 91131; 65 kDa), p38 MAPK (CST; Rabbit; 1:1,000 dilution; cat. no. 8690; 40 kDa), p-p38 MAPK (CST; Rabbit; 1:1,000 dilution; #4511, 43 kDa), Bcl-2 (Abcam; Rabbit, 1:2,000 dilution; cat. no. ab182858; 26 kDa), Bax (Abcam; Rabbit; 1:1,000; cat. no. ab32503; 21 kDa), cleaved-caspase-3 (CST; Rabbit; 1:1,000 dilution; cat. no. 9664; 17 kDa) and GAPDH (Abcam, Mouse, 1:5,000 dilution; cat. no. ab8245; 36 kDa). The membrane was then washed by tris-buffered saline with 0.05% Tween-20 (TBST) and cultivated with HRP-conjugated goat polyclonal anti-rabbit secondary antibody IgG H&L (Abcam; 1:3,000 dilution; cat. no. ab97051) and HRP-conjugated goat anti-mouse secondary antibody IgG H&L (Abcam; 1:3,000 dilution; cat. no. ab205719) at 37˚C for 1 h. The membrane was immersed in ECL Luminous liquid (R30199; 100 ml, Pierce; Thermo Fisher Scientific, Inc.) using a GelDoc XR Biorad (Bio-Rad Laboratories, Inc.); the gray value of each special band on the image was analyzed by ImageJ software v1.8 (National Institute of Health).

Statistical analysis. SPSS 20.0 (IBM Corp.) was used for statistical analysis. The measurement data are expressed as the mean ± standard deviation. The comparison among groups was accomplished by one-way analysis of variance and Tukey's post-hoc test was used. P<0.05 was considered to indicate a statistically significant difference.

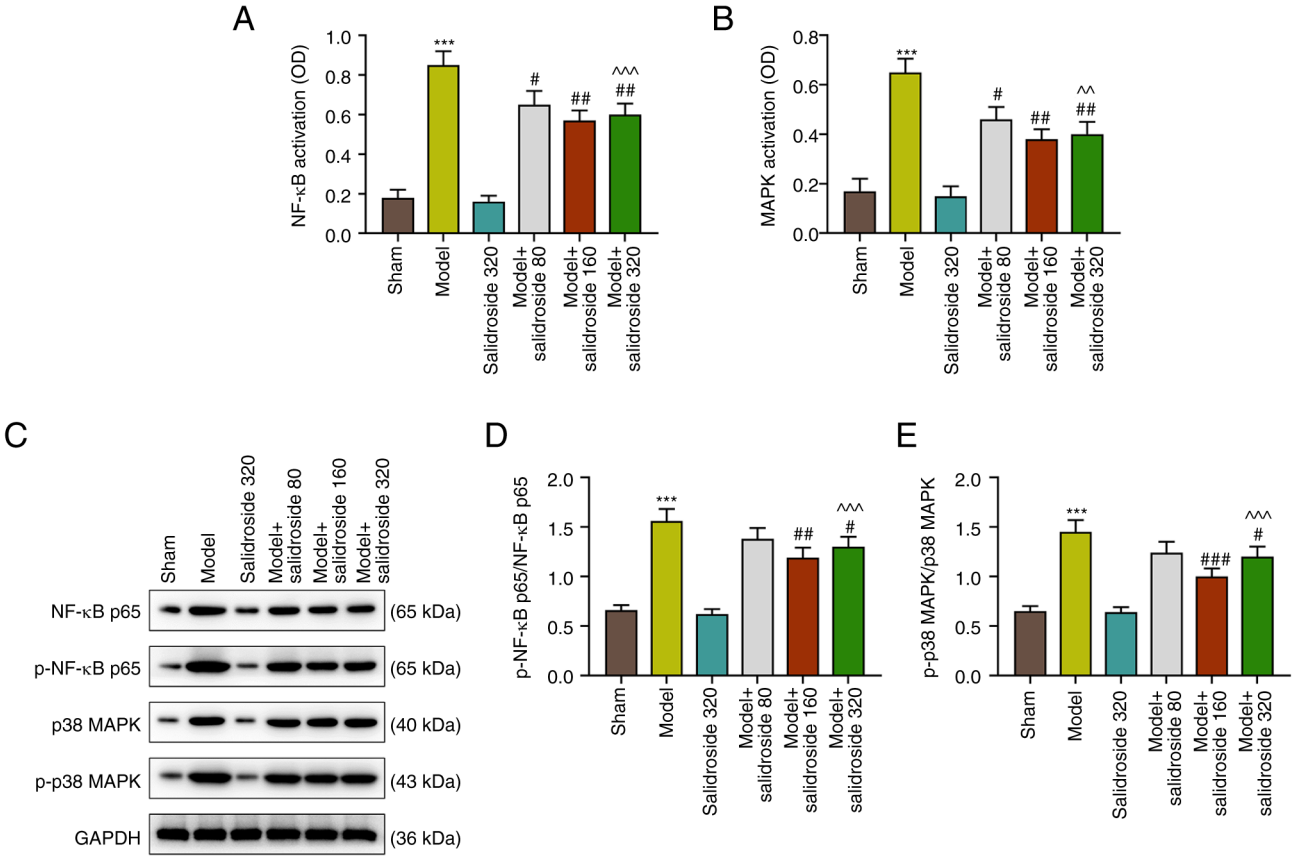

Figure 3. Salidroside affects the activation of NF-κB and p38 MAPK pathways in a septic model. (A) The NF-κB and (B) p38 MAPK signaling pathways activation was detected by ELISA. (C) Western blotting was performed to determine the protein expressions of (D) NF-κB p65 and (E) p38 MAPK. GAPDH was served as the internal reference. The data are presented as the mean ± standard deviation of three independent experiments; ***P<0.001 vs. sham; $^{\#}$P<0.05; $^{\#\#}$P<0.01; $^{\#\#\#}$P<0.001 vs. model; $^{\wedge\wedge}$P<0.01; $^{\wedge\wedge\wedge}$P<0.001 vs. salidroside (320 mg/kg).

Results

Salidroside mitigates the injury of ileum tissues and intestinal permeability induced by a septic model and reversely regulated ileum tissue cytokines. It can be seen from Fig. 1A that in septic model group, the injury of ileum tissue was the severest, the intestinal villi became shorter and thicker, the arrangement was disordered, the epithelial space of intestinal villi was clearly and continuously broken, the epithelial layer and lamina propria declined and the capillary congestion and hemorrhage of lamina propria could be observed. By contrast, the ileum tissue injury was effectively mitigated in the model + salidroside (80, 160, 320 mg/kg) group, especially in the model + salidroside (160 mg/kg) group. Fig. 1B shows that FD4 concentration was significantly higher in septic model group compared with the sham group (P<0.001; Fig. 1B). Compared with the model group, FD4 concentration was decreased evidently in in the model + salidroside (80, 160, 320 mg/kg) group (P<0.001; Fig. 1B), especially in the model + salidroside (160 mg/kg) group. The ileum tissue cytokine levels (Fig. 1C-F) revealed that the levels of IL-17, IL-6 and TNF-α in septic model group notably exceeded those in sham group (P<0.001; Fig. 1C, D and F) and IL-17, IL-6 and TNF-α levels in sepsis group were decreased by salidroside (80, 160, 320 mg/kg; P<0.01; Fig. 1C, D and F), especially salidroside (160 mg/kg). The IL-13 level in sham group was evidently reduced by septic model (P<0.001, 1E). Compared with the model group, IL-13 level was clearly increased in model + salidroside (80, 160, 320 mg/kg) group, especially in the model + salidroside (160 mg/kg) group. These data demonstrated that salidroside partly reversed the effect of septic model, alleviating the ileum tissue injury and intestinal permeability and decreasing the levels of inflammation-related cytokines.

Salidroside attenuates the decreased in the levels of intestinal tight junction proteins in the septic model. The intestinal mucosa is a physical and metabolic barrier, regulated by epithelial junction complexes known as tight junctions. This barrier function is reflected by the intestinal permeability. Thus, the levels of intestinal tight junction proteins: ZO-1, occludin and claudin-5 were further detected in septic mice. The results showed that the levels of ZO-1, occludin and claudin-5 were decreased in septic model, which was attenuated by salidroside (80, 160, 320 mg/kg) (P<0.01; Fig. 2A-D), especially salidroside at 160 mg/kg.

Salidroside suppresses the activation of NF-κB and p38 MAPK pathways in the septic model. As shown in Fig. 3A and B, the NF-κB and p38 MAPK signaling pathways were activated in the septic model (P<0.001; Fig. 3A and B), which were then inhibited by salidroside (80, 160, 320 mg/kg) (P<0.01; Fig. 3A and B), especially salidroside at 160 mg/kg. Fig. 3C to E show that the protein expressions of p-NF-κB p65/NF-κB p65 and p-p38 MAPK/p38 MAPK were evidently augmented

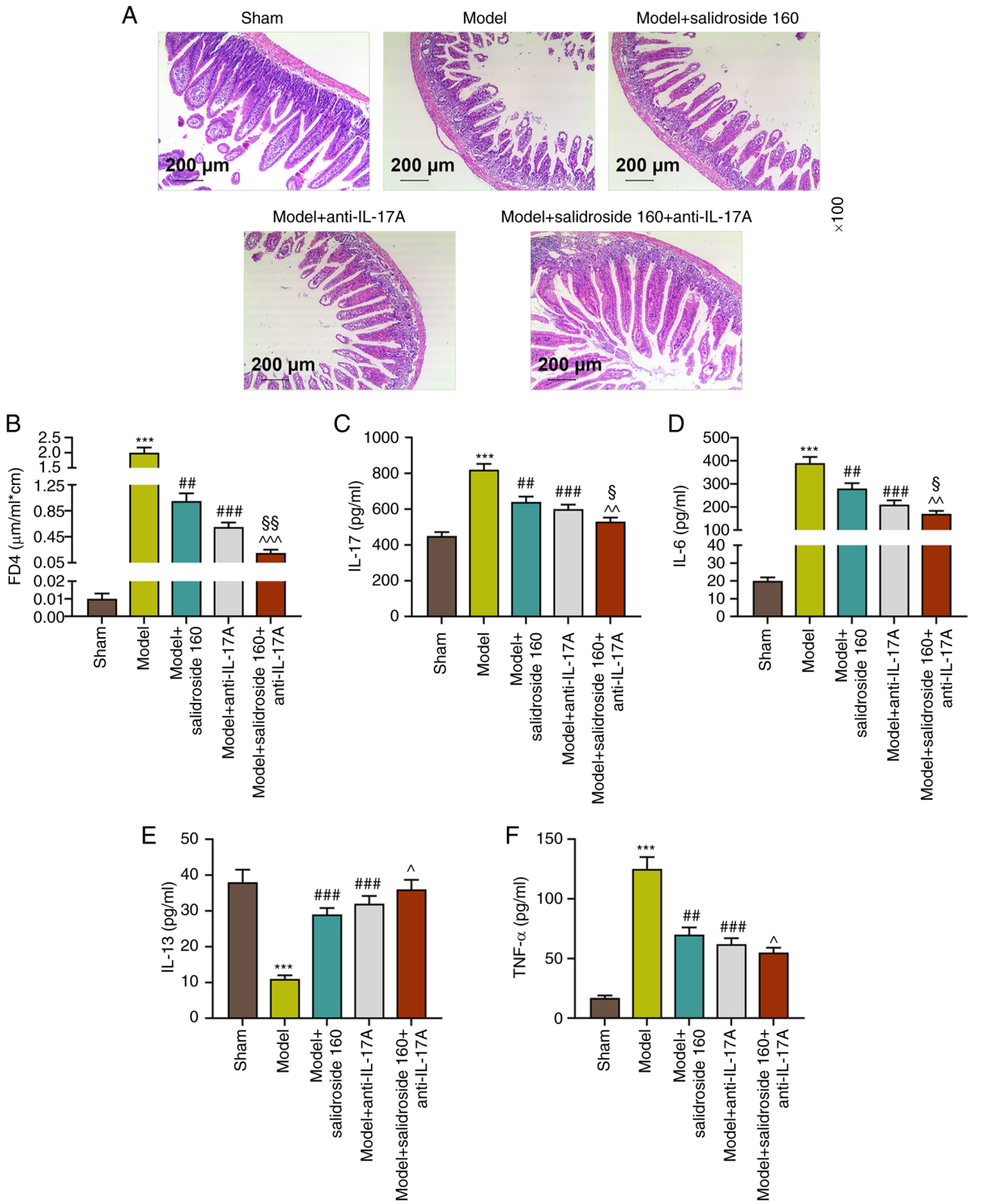

Figure 4. Anti-IL-17A further affects the ileum tissue injury and intestinal permeability and regulated ileum tissue cytokines in sepsis mice treated with salidroside. (A) The ileum tissues of mice were examined by histopathological examination. (B) FD4 concentration was measured by fluorospectrophotometer to detect intestinal permeability. (C) IL-17, (D) IL-6, (E) IL-13 and (F) TNF-α levels in ileum were detected by ELISA. The data are presented as the mean ± standard deviation of three independent experiments; ***P<0.001 vs. sham; $^{\#\#}$P<0.01; $^{\#\#\#}$P<0.001 vs. model; ^P<0.05; ^^P<0.01; ^^^P<0.001 vs. model + salidroside (160 mg/kg); §P<0.05; §§P<0.01 vs. model + anti-IL-17A. FD4, fluorescein isothiocyanate-dextran.

in septic model mice (P<0.001; Fig. 3C-E). However, the two expressions were then sharply downregulated by salidroside (80, 160, 320 mg/kg; P<0.001; Fig. 3C-E), especially salidroside at 160 mg/kg. The expression levels of Bax and Bcl-2 were also determined, as they are members of the Bcl-2 family involved in the intrinsic apoptotic pathway. The

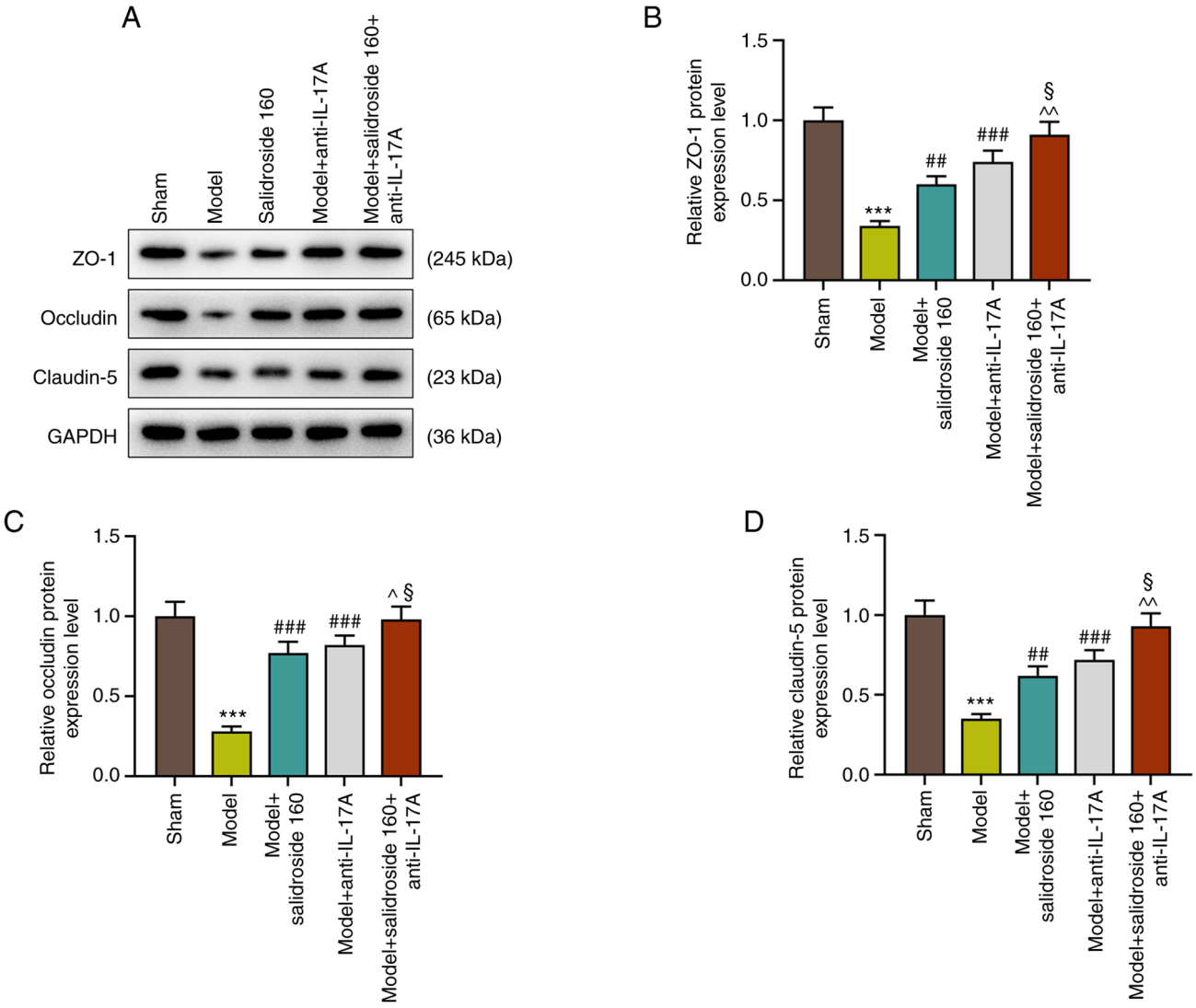

Figure 5. Anti-IL-17A further attenuates the decreases in the levels of intestinal tight junction proteins in sepsis mice treated with salidroside. (A-D) The levels of intestinal tight junction proteins (B) ZO-1, (C) occludin and (D) claudin-5 were detected by western blotting. GAPDH was served as the internal reference. The data are presented as the mean ± standard deviation of three independent experiments; ***P<0.001 vs. sham; $^{\#\#}$P<0.01; $^{\#\#\#}$P<0.001 vs. model; $^{\wedge}$P<0.05; $^{\wedge\wedge}$P<0.01 vs. model + salidroside (160 mg/kg); §P<0.05 vs. model + anti-IL-17A. ZO-1, zonula occludens-1.

results showed that the level of Bcl-2 was decreased, while those of Bax and cleaved-caspase-3 were elevated in septic model (P<0.001; Fig. S1A-D); however, salidroside (80, 160, 320 mg/kg) increased the level of Bcl-2 and decreased the levels of Bax and cleaved-caspase-3 in septic model (P<0.001; Fig. S1A-D), especially salidroside at 160 mg/kg.

Thus, salidroside suppressed activation of NF-κB and p38 MAPK pathways in the septic model. Considering that salidroside at 160 mg/kg generated the most effective effect, this dosage was therefore selected in the following experiments.

Anti-IL-17A further alleviates the ileum tissue injury and intestinal permeability and reversely regulates ileum tissue cytokines in sepsis mice treated with salidroside. The present study used IL-17A antagonist to verify the protective mechanism of salidroside in intestinal barrier dysfunction of sepsis mice. Fig. 4A shows that septic model-induced ileum tissue injury was mitigated in both the model + anti-IL-17A group and the model + salidroside (160 mg/kg) group and the mitigative effect was strengthened in model + salidroside (160 mg/kg) + anti-IL-17A group, resulting in the ileum tissue in a condition close to that in the sham group. In addition, FD4 concentration was much lower in model + anti-IL-17A group compared with the septic model group (P<0.001; Fig. 4B) and that was further diminished in model + salidroside (160 mg/kg) + anti-IL-17A group compared with that in model + anti-IL-17A group (P<0.01; Fig. 4B). In addition, the ileum tissue cytokine levels of IL-17, IL-6 and TNF-α that had been increased in septic model group were decreased in the model + anti-IL-17A group (P<0.001; Fig. 4C, D and F) and salidroside (160 mg/kg) further decreased the levels in model + anti-IL-17A group. Anti-IL-17A had a promoting effect on IL-13 levels. From the above data, anti-IL-17A could mitigate the ileum tissue injury and intestinal permeability induced by septic model and reversely modulated ileum tissue cytokines.

Anti-IL-17A further attenuates the decreased in the levels of intestinal tight junction proteins in sepsis mice treated with

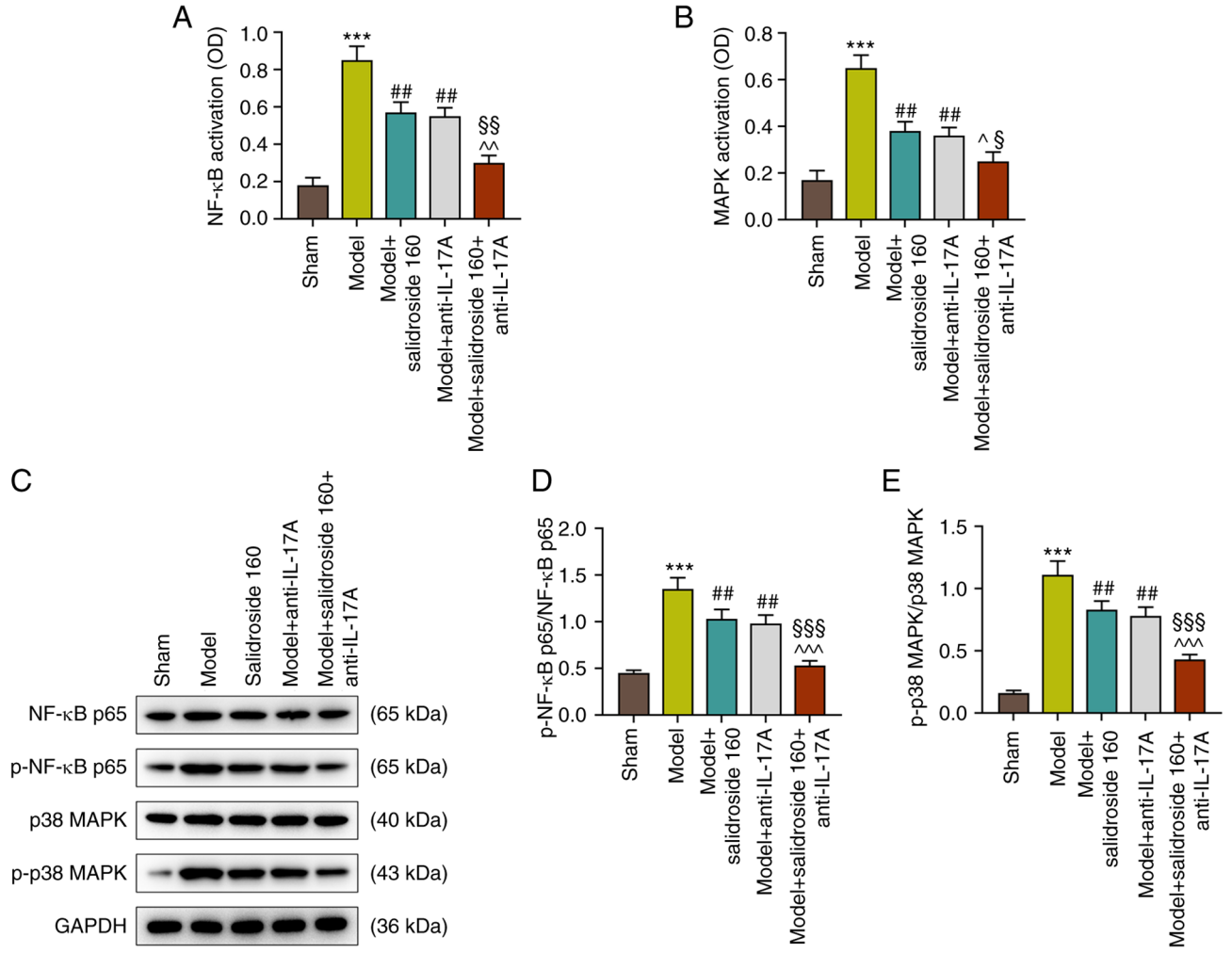

Figure 6. Anti-IL-17A further affects the activated NF-κB and p38 MAPK pathways in sepsis mice treated with salidroside. The activation of (A) NF-κB and (B) p38 MAPK signaling pathways was examined by ELISA. (C) Western blotting was performed to detect the (D) p-NF-κB p65/NF-κB p65 and (E) -p38 MAPK/p38 MAPK protein expressions and GAPDH was served as the internal reference. The data were presented as the mean ± standard deviation of three independent experiments; ***P<0.001 vs. sham; $^{\#\#}$P<0.01 vs. model; $^{\wedge}$P<0.05; $^{\wedge\wedge}$P<0.01 vs. salidroside (160 mg/kg), $^{\wedge\wedge\wedge}$P<0.001; §P<0.05; §§P<0.01 vs. model + anti-IL-17A, §§§P<0.001..

salidroside. The results showed that anti-IL-17A increased the levels of ZO-1, occludin and claudin-5 in septic model and further promoted the effect of salidroside (160 mg/kg) in septic model (P<0.001; Fig. 5A-D).

Anti-IL-17A further inhibits the activated NF-κB and p38 MAPK pathways in sepsis mice treated with salidroside. According to Fig. 4A and B, as with salidroside (160 mg/kg), anti-IL-17A also suppressed the septic model-induced NF-κB and p38 MAPK signaling pathways activation (P<0.01; Fig. 6A and B) and anti-IL-17A combined with salidroside (160 mg/kg) was more effective than anti-IL-17A alone (P<0.05; Fig. 6A and B). Similarly, the p-NF-κB p65/NF-κB p65 and p-p38 MAPK/p38 MAPK protein expressions in septic model group were decreased after the treatment with anti-IL-17A (P<0.01; Fig. 6C-E) and the effect of anti-IL-17A was reinforced when combined with salidroside at 160 mg/kg (P<0.001; Fig. 6C-E). As a consequence, anti-IL-17A could counteract the effect of septic model, inhibiting the activated NF-κB and p38 MAPK signaling pathways. Moreover, anti-IL-17A and salidroside (160 mg/kg) in combination were more effective.

The results showed that anti-IL-17A elevated the level of Bcl-2 and decreased the levels of Bax and cleaved-caspase-3 in septic model (P<0.001; Fig. S2A-D). Moreover, anti-IL-17A in combination with salidroside further elevated the level of Bcl-2 and decreased the levels of Bax and cleaved-caspase-3 in septic model (P<0.001, Fig. S2A-D). Finally, the salidroside-associated mechanisms of action against the sepsis model to mitigate the inflammation is shown in Fig. S3.

Discussion

Sepsis is a systemic inflammatory response syndrome, mainly caused by infection or suspected infectious factors (32). The intestinal mucosal immune barrier is composed of intestinal-associated lymphoid tissue and diffused immune cells, which serve an important role in protecting intestinal function and regulating the occurrence and development of sepsis (33). Salidroside, a type of phenylethanol compound extracted from *Rhodiola*, has been proved to be able to rescue mice from experimental sepsis induced by CLP through anti-inflammatory and anti-apoptosis effects (34). In addition,

salidroside alleviates myocarditis induced by sepsis in rats through regulation of IGF-1/PI3K/Akt/GSK-3β signaling (35).

The present study established a sepsis mouse model to identify the effect of salidroside on intestinal mucosal barrier in mice. The results showed that after the treatment with salidroside, intestinal villi presented normal basic morphology and were arranged regularly, the epithelial space was obviously dilated, capillary congestion was observed and the lamina propria was still intact. Adherens junctions and intestinal tight junction proteins, made up of occludin, claudin and ZO-1, serve a crucial role for protecting the intestinal mucosal barrier (36-38). This barrier function is reflected by the intestinal permeability. The intestinal permeability was decreased while the expressions of intestinal tight junction proteins were increased by the administration of salidroside. Thus, salidroside could prevent the increase in mucosal permeability and increase the expressions of tight junctional proteins, inhibiting intestinal damage and protecting the intestinal mucosal barrier during sepsis.

The main pathophysiological process of sepsis is excess activation of inflammatory response caused by pathogen infection and the secondary immune dysfunction or immunosuppression (39). Human immune responses to severe infections are mediated mainly by the primary proinflammatory cytokine TNF-α and by the secondary proinflammatory mediators IL-6 and IL-17 (40). TNF-α and IL-6 are both considered as notable elements in the cytokine network during sepsis (40) and IL-17 is upregulated in both clinical and experimental sepsis (41). Studies show that IL-6 concentration in plasma could be a new biomarker for the sepsis diagnosis (42) and the neutralization of TNF-α could prolong survival time of patients with moderate/severe CLP sepsis (43). On the other hand, the anti-inflammatory cytokine IL-13 neutralizes the excessive production of proinflammatory cytokines and may induce a state of immunosuppression in patients with sepsis (44). Previous studies report that salidroside attenuates the levels of TNF-α and IL-6 in LPS-induced myocardial injury (45) and the expression of IL-17 is decreased following salidroside treatment in heart failure left ventricle (46). In addition, salidroside suppresses the upregulation of IL-13 in bronchoalveolar lavage fluids and lung tissues of ovalbumin-induced asthma mice model (47). The present study revealed that the levels of TNF-α, IL-6 and IL-17 were upregulated and IL-13 level was downregulated by septic model. Salidroside treatment partially reversed the effects of septic model, which increased IL-13 level yet decreased the levels of TNF-α, IL-6 and IL-17, showing alleviative effects on the septic model-induced inflammation in the ileum tissues of mice. A previous report indicates that post-treatment salidroside attenuates CLP-induced increase in the serum levels of inflammatory factors, including plasma TNF-α and IL-6, -1β and-10 in septic rats and also significantly attenuate the activation of NF-κB and increase the release of peroxisome proliferator-activated receptor γ in the lung tissue (13). Accumulating evidence also reports the inhibitory effects of natural products on CLP-induced sepsis. Shenfu decoction may serve a protective role in sepsis by inhibiting inflammatory response and gut barrier damage in rats with CLP-induced sepsis (48). Astragaloside IV protects intestinal epithelium from sepsis-induced barrier dysfunction through blocking RhoA/NLRP3 inflammasome signal pathway (49). Sodium tanshinone IIA sulfonate attenuates cardiac dysfunction and improves survival of rats with CLP-induced sepsis (50).

It has been reported that glucosamine attenuates lung injury and inflammation by suppressing the MAPK and NF-κB activation (51) and maresin 1 alleviates acute kidney injury in septic mice by blocking the NF-κB/STAT3/MAPK pathways (52). It is also reported that MAPK/NF-κB serves important roles in the inflammatory response and apoptosis regulation (53-55). Increase of Bcl-2 or inhibition of caspases also lead to an elevated survival in animal models of sepsis (56). Previous studies indicate that salidroside regulates the MAPK/NF-κB pathway (9,21,57). IL-17, which has the ability to induce the activation of NF-κB and MAPK pathways in rheumatoid arthritis synovial fibroblasts and human colonic myofibroblasts (58,59), has also been reported to promote the sepsis-induced cardiac dysfunction via the NF-κB and MAPK pathways (60). Additionally, salidroside protects mice from CLP-induced sepsis by exerting its anti-inflammatory and anti-apoptosis effects (34). In the present study, salidroside also exerted anti-inflammatory and anti-apoptosis effects on septic mice. The current study corroborated that septic model-activated MAPK/NF-κB signaling pathways were suppressed by IL-17 regulated by the treatment of salidroside.

In brief, the results demonstrated that salidroside reduced inflammation to protect against intestinal barrier dysfunction in septic mice by downregulating IL-17, thereby suppressing the NF-κB and p38 MAPK signaling pathways, which thus could be a therapeutic option in current therapy of intestinal barrier dysfunction during sepsis.

Acknowledgements

Not applicable.

Funding

No funding was received.

Availability of data and materials

The datasets used and/or analyzed during the current study are available from the corresponding author on reasonable request.

Authors' contributions

RL made substantial contributions to conception and design of the present study, drafted the manuscript and critically revised it for important intellectual content. PZ, JW and KF performed data acquisition, data analysis and interpretation. RL, PZ, JW and KF confirm the authenticity of all the raw data. All authors read and approved the final manuscript.

Ethics approval and consent to participate

All animal experiments, performed in Nanfang Hospital following the guidelines of the China Council on Animal Care and Use, were permitted by the Committee of Experimental

Animals of Nanfang Hospital (approval no. S201709024). The pain and discomfort to the animals were minimized.

Patient consent for publication

Not applicable.

Competing interests

The authors declare that they have no competing interests.

References

1. Shankar-Hari M, Phillips GS, Levy ML, Seymour CW, Liu VX, Deutschman CS, Angus DC, Rubenfeld GD and Singer M: Developing a new definition and assessing new clinical criteria for septic shock: For the third international consensus definitions for sepsis and septic shock (Sepsis-3). JAMA 315: 775-787, 2016.
2. Deutschman CS and Tracey KJ: Sepsis: Current dogma and new perspectives. Immunity 40: 463-475, 2014.
3. Hawiger J, Veach RA and Zienkiewicz J: New paradigms in sepsis: From prevention to protection of failing microcirculation. J Thromb Haemost 13: 1743-1756, 2015.
4. Adib-Conquy M and Cavaillon JM: Host inflammatory and anti-inflammatory response during sepsis. Pathol Biol (Paris) 60: 306-313, 2012 (In French).
5. de Medina FS, Romero-Calvo I, Mascaraque C and Martínez-Augustin O: Intestinal inflammation and mucosal barrier function. Inflamm Bowel Dis 20: 2394-2404, 2014.
6. Panossian A, Wikman G and Sarris J: Rosenroot (Rhodiola rosea): Traditional use, chemical composition, pharmacology and clinical efficacy. Phytomedicine 17: 481-493, 2010.
7. Xue F, Yang M and Ma L: Microbial synthesis of salidroside. Sheng Wu Gong Cheng Xue Bao 35: 1184-1192, 2019.
8. Zhou F, Ju J, Fang Y, Fan X, Yan S, Wang Q, Wei P, Duan F, Miao F, Hu Z and Wang M: Salidroside protected against MPP(+)-induced Parkinson's disease in PC12 cells by inhibiting inflammation, oxidative stress and cell apoptosis. Biotechnol Applied Biochem 66: 247-253, 2019.
9. Xu N, Huang F, Jian C, Qin L, Lu F, Wang Y, Zhang Z and Zhang Q: Neuroprotective effect of salidroside against central nervous system inflammation-induced cognitive deficits: A pivotal role of sirtuin 1-dependent Nrf-2/HO-1/NF-κB pathway. Phytother Res 33: 1438-1447, 2019.
10. Zhong Z, Han J, Zhang J, Xiao Q, Hu J and Chen L: Pharmacological activities, mechanisms of action, and safety of salidroside in the central nervous system. Drug Des Devel Ther 12: 1479-1489, 2018.
11. Hu R, Wang MQ, Ni SH, Wang M, Liu LY, You HY, Wu XH, Wang YJ, Lu L and Wei LB: Salidroside ameliorates endothelial inflammation and oxidative stress by regulating the AMPK/NF-κB/NLRP3 signaling pathway in AGEs-induced HUVECs. Eur J Pharmacol 867: 172797, 2020.
12. Zhong ZF, Han J, Zhang JZ, Xiao Q, Chen JY, Zhang K, Hu J and Chen LD: Neuroprotective effects of salidroside on cerebral ischemia/reperfusion-induced behavioral impairment involves the dopaminergic system. Front Pharmacol 10: 1433, 2019.
13. Liu MW, Su MX, Qin LF, Liu X, Tian ML, Zhang W and Wang YH: Effect of salidroside on lung injury by upregulating peroxisome proliferator-activated receptor γ expression in septic rats. Exp Ther Med 7: 1446-1456, 2014.
14. Yasuda K, Takeuchi Y and Hirota K: The pathogenicity of Th17 cells in autoimmune diseases. Semin Immunopathol 41: 283-297, 2019.
15. Gu C, Wu L and Li X: IL-17 family: Cytokines, receptors and signaling. Cytokine 64: 477-485, 2013.
16. Monin L and Gaffen SL: Interleukin 17 family cytokines: Signaling mechanisms, biological activities, and therapeutic implications. Cold Spring Harbor perspect Biol 10: a028522, 2018.
17. Kuwabara T, Ishikawa F, Kondo M and Kakiuchi T: The role of IL-17 and related cytokines in inflammatory autoimmune diseases. Mediators Inflamm 2017: 3908061, 2017.
18. Brembilla NC, Senra L and Boehncke WH: The IL-17 family of cytokines in psoriasis: IL-17A and beyond. Front Immunol 9: 1682, 2018.
19. Lubberts E: IL-17/Th17 targeting: On the road to prevent chronic destructive arthritis? Cytokine 41: 84-91, 2008.
20. Lubberts E, Koenders MI, Oppers-Walgreen B, van den Bersselaar L, Coenen-de Roo CJ, Joosten LA and van den Berg WB: Treatment with a neutralizing anti-murine interleukin-17 antibody after the onset of collagen-induced arthritis reduces joint inflammation, cartilage destruction, and bone erosion. Arthritis Rheum 50: 650-659, 2004.
21. Li J, Kong P, Chen C, Tang J, Jin X, Yan J and Wang Y: Targeting IL-17A improves the dysmotility of the small intestine and alleviates the injury of the interstitial cells of cajal during sepsis. Oxid Med Cell Longev 2019: 1475729, 2019.
22. Lee JS, Tato CM, Joyce-Shaikh B, Gulen MF, Cayatte C, Chen Y, Blumenschein WM, Judo M, Ayanoglu G, McClanahan TK, *et al*: Interleukin-23-independent IL-17 production regulates intestinal epithelial permeability. Immunity 43: 727-738, 2015.
23. Wei L, Xiong H, Li W, Li B and Cheng Y: Upregulation of IL-6 expression in human salivary gland cell line by IL-17 via activation of p38 MAPK, ERK, PI3K/Akt, and NF-κB pathways. J Oral Pathol Med 47: 847-855, 2018.
24. Chang SL, Hsiao YW, Tsai YN, Lin SF, Liu SH, Lin YJ, Lo LW, Chung FP, Chao TF, Hu YF, *et al*: Interleukin-17 enhances cardiac ventricular remodeling via activating MAPK pathway in ischemic heart failure. J Mol Cell Cardiol 122: 69-79, 2018.
25. Wei L, Liu M, Xiong H and Peng B: Up-regulation of IL-23 expression in human dental pulp fibroblasts by IL-17 via activation of the NF-κB and MAPK pathways. Int Endod J 51: 622-631, 2018.
26. Johansen C, Kragballe K, Westergaard M, Henningsen J, Kristiansen K and Iversen L: The mitogen-activated protein kinases p38 and ERK1/2 are increased in lesional psoriatic skin. Br J Dermatol 152: 37-42, 2005.
27. Chen H, Wang X, Yan X, Cheng X, He X and Zheng W: LncRNA MALAT1 regulates sepsis-induced cardiac inflammation and dysfunction via interaction with miR-125b and p38 MAPK/NFκB. Int Immunopharmacol 55: 69-76, 2018.
28. Cai X, Chen Y, Xie X, Yao D, Ding C and Chen M: Astaxanthin prevents against lipopolysaccharide-induced acute lung injury and sepsis via inhibiting activation of MAPK/NF-κB. Am J Transl Res 11: 1884-1894, 2019.
29. Lan KC, Chao SC, Wu HY, Chiang CL, Wang CC, Liu SH and Weng TI: Salidroside ameliorates sepsis-induced acute lung injury and mortality via downregulating NF-κB and HMGB1 pathways through the upregulation of SIRT1. Sci Rep 7: 12026, 2017.
30. Zhang XR, Fu XJ, Zhu DS, Zhang CZ, Hou S, Li M and Yang XH: Salidroside-regulated lipid metabolism with down-regulation of miR-370 in type 2 diabetic mice. Eur J Pharmacol 779: 46-52, 2016.
31. Yang ZR, Wang HF, Zuo TC, Guan LL and Dai N: Salidroside alleviates oxidative stress in the liver with non-alcoholic steatohepatitis in rats. BMC Pharmacol Toxicol 17: 16, 2016.
32. Uhle F, Lichtenstern C, Brenner T and Weigand MA: Pathophysiology of sepsis. Anasthesiol Intensivmed Notfallmed Schmerzther 50: 114-122, 2015.
33. Hu Q, Ren H, Li G, Wang D, Zhou Q, Wu J, Zheng J, Huang J, Slade DA, Wu X and Ren J: STING-mediated intestinal barrier dysfunction contributes to lethal sepsis. EBioMedicine 41: 497-508, 2019.
34. Liu S, Yu X, Hu B, Zou Y, Li J, Bo L and Deng X: Salidroside rescued mice from experimental sepsis through anti-inflammatory and anti-apoptosis effects. J Surg Res 195: 277-283, 2015.
35. He H, Chang X, Gao J, Zhu L, Miao M and Yan T: Salidroside mitigates sepsis-induced myocarditis in rats by regulating IGF-1/PI3K/Akt/GSK-3β signaling. Inflammation 38: 2178-2184, 2015.
36. Liu F, Liu J, Liu Y, Zhang Y and Ding X: Shen-Fu Decoction could ameliorate intestinal permeability by regulating the intestinal expression of tight junction proteins and p-VASP in septic rats. J Ethnopharmacol 268: 113562, 2021.
37. Wang L, Cui YL, Zhang Z, Lin ZF and Chen DC: Rhubarb monomers protect intestinal mucosal barrier in sepsis via junction proteins. Chin Med J (Engl) 130: 1218-1225, 2017.
38. Li Y, Guo R, Zhang M, Chen P, Li J and Sun Y: Protective effect of emodin on intestinal epithelial tight junction barrier integrity in rats with sepsis induced by cecal ligation and puncture. Exp Ther Med 19: 3521-3530, 2020.
39. Kumar V and Sharma A: Innate immunity in sepsis pathogenesis and its modulation: New immunomodulatory targets revealed. J Chemother 20: 672-683, 2008.

40. Cao YZ, Tu YY, Chen X, Wang BL, Zhong YX and Liu MH: Protective effect of Ulinastatin against murine models of sepsis: Inhibition of TNF-α and IL-6 and augmentation of IL-10 and IL-13. Exp Toxicol Pathol 64: 543-547, 2012.
41. Lv R, Zhao J, Lei M, Xiao D, Yu Y and Xie J: IL-33 attenuates sepsis by inhibiting IL-17 receptor signaling through upregulation of SOCS3. Cell Physiol Biochem 42: 1961-1972, 2017.
42. Franco DM, Arevalo-Rodriguez I, Roqué IFM, Oleas NG, Nuvials X and Zamora J: Plasma interleukin-6 concentration for the diagnosis of sepsis in critically ill adults. Cochrane Database Syst Rev 4: CD011811, 2019.
43. Newham P, Ross D, Ceuppens P, Das S, Yates JW, Betts C, Reens J, Randall KJ, Knight R and McKay JS: Determination of the safety and efficacy of therapeutic neutralization of tumor necrosis factor-α (TNF-α) using AZD9773, an anti-TNF-α immune Fab, in murine CLP sepsis. Inflamm Res 63: 149-160, 2014.
44. Collighan N, Giannoudis PV, Kourgeraki O, Perry SL, Guillou PJ and Bellamy MC: Interleukin 13 and inflammatory markers in human sepsis. Br J Surg 91: 762-768, 2004.
45. Chen L, Liu P, Feng X and Ma C: Salidroside suppressing LPS-induced myocardial injury by inhibiting ROS-mediated PI3K/Akt/mTOR pathway in vitro and in vivo. J Cell Mol Med 21: 3178-3189, 2017.
46. Hsiao YW, Tsai YN, Huang YT, Liu SH, Lin YJ, Lo LW, Hu YF, Chung FP, Lin SF, Chang SL, *et al*: Rhodiola crenulata reduces ventricular arrhythmia through mitigating the activation of IL-17 and inhibiting the MAPK signaling pathway. Cardiovasc Drugs Ther 35: 889-900, 2020.
47. Yan GH and Choi YH: Salidroside attenuates allergic airway inflammation through negative regulation of nuclear factor-kappa B and p38 mitogen-activated protein kinase. J Pharmacol Sci 126: 126-135, 2014.
48. Liu J, Liu F, Liang T, Cao P, Li J, Zhang Y and Liu Y: Efficacy of Shenfu decoction on sepsis in rats with condition induced by cecal ligation and puncture. J Tradit Chin Med 40: 621-628, 2020.
49. Xie S, Yang T, Wang Z, Li M, Ding L, Hu X and Geng L: Astragaloside IV attenuates sepsis-induced intestinal barrier dysfunction via suppressing RhoA/NLRP3 inflammasome signaling. Int Immunopharmacol 78: 106066, 2020.
50. Meng ZJ, Wang C, Meng LT, Bao BH, Wu JH and Hu YQ: Sodium tanshinone IIA sulfonate attenuates cardiac dysfunction and improves survival of rats with cecal ligation and puncture-induced sepsis. Chin J Nat Med 16: 846-855, 2018.
51. Hwang JS, Kim KH, Park J, Kim SM, Cho H, Lee Y and Han IO: Glucosamine improves survival in a mouse model of sepsis and attenuates sepsis-induced lung injury and inflammation. J Biol Chem 294: 608-622, 2019.
52. Sun S, Wang J, Wang J, Wang F, Yao S and Xia H: Maresin 1 mitigates sepsis-associated acute kidney injury in mice via inhibition of the NF-κB/STAT3/MAPK pathways. Front Pharmacol 10: 1323, 2019.
53. Chang NC, Yeh CT, Lin YK, Hu P, Kuo KT, Fong IH, Kounis NG, Hu P and Hung MY: Garcinol attenuates lipoprotein(a)-induced oxidative stress and inflammatory cytokine production in ventricular cardiomyocyte through α7-nicotinic acetylcholine receptor-mediated inhibition of the p38 MAPK and NF-κB signaling pathways. Antioxidants (Basel) 10: 461, 2021.
54. Chen Q, Lu H, Duan C, Zhu X, Zhang Y, Li M and Zhang D: PDCD4 simultaneously promotes microglia activation via PDCD4-MAPK-NF-κB positive loop and facilitates neuron apoptosis during neuroinflammation. Inflammation 45: 234-252, 2022.
55. Jarisarapurin W, Kunchana K, Chularojmontri L and Wattanapitayakul SK: Unripe carica papaya protects methylglyoxal-invoked endothelial cell inflammation and apoptosis via the suppression of oxidative stress and Akt/MAPK/NF-κB signals. Antioxidants (Basel) 10: 1158, 2021.
56. Weber SU, Schewe JC, Putensen C, Stüber F and Schröder S: Apoptosis as a pathomechanism in sepsis. Anaesthesist 53: 59-65, 2004 (In German).
57. Li R, Guo Y, Zhang Y, Zhang X, Zhu L and Yan T: Salidroside ameliorates renal interstitial fibrosis by inhibiting the TLR4/NF-κB and MAPK signaling pathways. Int J Mol Sci 20: 1103, 2019.
58. Hata K, Andoh A, Shimada M, Fujino S, Bamba S, Araki Y, Okuno T, Fujiyama Y and Bamba T: IL-17 stimulates inflammatory responses via NF-kappaB and MAP kinase pathways in human colonic myofibroblasts. Am J Physiol Gastrointestinal Liver Physiol 282: G1035-G1044, 2002.
59. Hwang SY, Kim JY, Kim KW, Park MK, Moon Y, Kim WU and Kim HY: IL-17 induces production of IL-6 and IL-8 in rheumatoid arthritis synovial fibroblasts via NF-kappaB- and PI3-kinase/Akt-dependent pathways. Arthritis Res Ther 6: R120-R128, 2004.
60. He S, Zhao J, Xu X, Cui X, Wang N, Han X, Guo Y and Liu Q: Uncovering the molecular mechanism of the Qiang-Xin 1 formula on sepsis-induced cardiac dysfunction based on systems pharmacology. Oxid Med Cell Longev 2020: 3815185, 2020.